Pharmaceutical Research, Vol. 23, No. 8, August 2006 (© 2006)
DOI: 10.1007/s11095-006-9010-9

Research Paper

Enhanced Transscleral Iontophoretic Transport with Ion-Exchange Membrane

S. Kevin Li,[1,2,3,4] Honggang Zhu,[1] and William I. Higuchi[1]

Received January 19, 2006; accepted March 14, 2006

Purpose. Transscleral iontophoresis has been recently re-examined for drug delivery to the back of the eye. In conventional iontophoresis, due to the relatively high electromobility of the endogenous competing ions (counterions) relative to that of the drug ion in the tissue barrier, the efficiency of iontophoretic drug delivery is generally low. The objective of the present study was to examine ion-exchange membrane-enhanced transscleral iontophoretic transport in which the ion-exchange membrane in series with the sclera can hinder the transport of the competing counterions and selectively allow the transport of the permeant across the sclera.

Methods. The physical properties of the Ionac ion-exchange membrane and excised rabbit sclera were determined in equilibrium uptake experiments and in passive and iontophoretic transport experiments with salicylate, tetraethylammonium, urea, and mannitol. Transscleral experiments with the ion-exchange membrane were conducted with salicylate and excised rabbit sclera *in vitro*. The contribution of electroosmosis to electrotransport during transscleral iontophoresis was assessed with urea and mannitol.

Results. The ion-exchange membrane is highly positively charged and has a small effective pore size. The sclera is relatively porous with a large effective pore size and low pore tortuosity. The sclera is also net negatively charged but this does not significantly affect the transport of small ions. A three-fold steady-state transscleral flux enhancement of salicylate was observed in ion-exchange membrane-enhanced iontophoresis over conventional transscleral iontophoresis without the membrane. Such enhancement was relatively independent of the applied electric current density and the thickness of the studied ion-exchange membrane assembly. Although the ion-exchange membrane altered transscleral electroosmosis, the contribution of electroosmosis to electrotransport was not significant.

Conclusions. The present study has demonstrated the potential of ion-exchange membranes for enhancing iontophoretic transport and drug delivery.

KEY WORDS: iontophoresis; ion-exchange membrane; salicylate; sclera; transscleral.

INTRODUCTION

Iontophoresis is a method to deliver a compound across a membrane with the assistance of an electric field (1,2). Because drug delivery to the back of the eye continues to be a challenge to pharmaceutical scientists and ophthalmologists, the utility and safety of ocular iontophoresis have recently been re-examined (3–7). In transscleral iontophoresis, a donor electrode containing the drug to be delivered into the eye is placed on the conjunctiva/sclera and, to complete an electrical circuit through the body, another electrode is placed on another body surface. The ions migrating from the donor electrode are ions of the same charge as the polarity of the donor electrode. The ions migrating from the body into the donor electrode (competing counterions) are usually endogenous ions having a charge opposite to the polarity of the electrode. The electric field enhances the transport of the permeant from the donor electrode across the tissue barriers, such as the conjunctiva, sclera, choroid, and retina, into the eye. When iontophoresis is operated under the constant electric current principle, the efficiency of iontophoretic transport is commonly assessed by the ratio of the current carried by the drug to the total electric current applied across the membrane. This ratio is known as the transference number (or transport number) of the drug (8–10). The optimal situation is achieved when the transference number of the drug approaches unity during iontophoresis.

Iontophoretic drug applications usually have low transference numbers (8,11). Typical iontophoretic transport efficiencies are below 50% because of (a) the relative high concentration of the endogenous competing counterions (e.g., NaCl) in the body and (b) the low electromobility of the drug ion compared with those of the small endogenous counterions. It is hypothesized that the efficiency of iontophoresis can be enhanced by the use of a synthetic ion-exchange membrane (12). In transscleral iontophoresis, an ion-exchange membrane can be incorporated between the donor electrode and the ocular tissue (the conjunctiva/sclera) surface to exclude

[1] Department of Pharmaceutics & Pharmaceutical Chemistry, University of Utah, Salt Lake City, Utah 84112, USA.
[2] Division of Pharmaceutical Sciences, College of Pharmacy, University of Cincinnati, Cincinnati, Ohio 45267, USA.
[3] Present address: College of Pharmacy, University of Cincinnati, 3225 Eden Avenue, Rm 136 HPB, Cincinnati, Ohio 45267, USA.
[4] To whom correspondence should be addressed. (e-mail:likv@uc.edu)

the transport of the current-carrying counterions from the eye. With the exclusion of these competing ions, iontophoretic drug delivery will be enhanced at the same applied electric current. In other words, the resistance of the combined ocular tissue and ion-exchange membrane system increases when the ion-exchange membrane is present due to transport hindrance to the competing counterions (from the eye into the ion-exchange membrane). The electric field applied across this combined membrane system increases to maintain the electric current at the set value, and the iontophoretic flux of the drug will be enhanced. It is believed that the use of ion-exchange membranes to enhance iontophoretic transport is especially favorable in ocular iontophoresis because the sclera, conjunctiva, and retinal epithelium have relatively high permeabilities and low electrical resistances compared to other biomembranes such as the skin. The exclusion of ion migration from the eye may be expected not only to enhance drug delivery, but also to reduce the variability of drug transport resulting from tissue variability when the transference number is enhanced and approaches unity.

The objectives of the present study were to (a) examine the feasibility of using an ion-exchange (permselective) membrane to enhance the efficiency (drug transference number) of iontophoretic transport with sclera and (b) characterize the properties of the ion-exchange membrane and sclera for mechanistic understanding of the iontophoretic transport system. Constant current transscleral iontophoresis experiments were conducted in a side-by-side diffusion cell *in vitro* with a negatively charged permeant salicylate, a positively charged ion-exchange membrane Ionac, and excised rabbit sclera. The experimental results with the ion-exchange membrane were then to be discussed in the light of previous theoretical results (13).

MATERIALS AND METHODS

Materials

^{3}H-mannitol, ^{14}C-urea, ^{14}C-tetraethyl ammonium (TEA), and ^{14}C-salicylate (SA) at >98% purity were purchased from PerkinElmer Life and Analytical Sciences (Boston, MA) and American Radiolabeled Chemicals, Inc. (St. Louis, MO) and checked for purity using the methods specified by the suppliers. Ion-exchange membrane Ionac (anion, MA-3475) was obtained from Sybron Chemicals (Birmingham, NJ). Phosphate buffered saline (PBS), pH 7.4, was prepared by PBS tablets purchased from Sigma-Aldrich, Co. (St. Louis, MO) and deionized distilled water. NaN_3 was added to PBS at 0.02% as bacteriostatic. Sodium salicylate (NaSA), pKa $\approx$ 3, was purchased from Sigma-Aldrich. NaSA solutions were prepared in deionized distilled water and the pH was adjusted to 7 with concentrated NaOH. Excised rabbit eyes were obtained from New Zealand white rabbits (3 to 4 kg, Western Oregon Rabbit Co., Philomath, OR) euthanized in other studies at the University of Utah Animal Resource Center under the approval of the Institutional Animal Care and Use Committee at the University of Utah. After the eye was separated from the rabbit and freed from adhering extraocular debris such as the conjunctiva and muscles, the sclera tissues of the superior and inferior temporal sections of the eye were taken. In the transport experiments, the diffusional area was a circular area of 0.5 cm diameter about 0.3 cm away from the limbus. In the membrane characterization experiments, sclera tissues of approximately 1×1 cm^2 were obtained from the same area. Unless otherwise specified, the retina was not removed from the sclera.

Theory and Equations

The efficiency of iontophoretic transport of a permeant is commonly assessed by the transference number (t_i) in constant current iontophoresis applications. The transference number equals the fraction of the current carried by the permeant, i.e., the ratio of the current carried by the permeant (I_i) to the total current carried by all ionic species (I_{total}) in the system:

$$t_i = \frac{I_i}{I_{total}} \tag{1}$$

and

$$t_i = \frac{|z_i|J_i}{\sum_j |z_j|J_j} \tag{2}$$

where J_i is the flux of species i (the permeant), J_j is the flux of ionic species j in the system, I_i is the current carried by ionic species i, I_{total} is the total current, z_i is the charge number of the ionic species i, and z_j is the charge number of ionic species j. The ionic species j represents both the oppositely charged counterions migrating into the donor from the receiver and the ions migrating into the receiver from the donor, including ionic species i. The flux of the permeant (J_i) is related to the current by:

$$J_i = \frac{t_i I_{total}}{A_D F|z_i|} \tag{3}$$

where A_D is the diffusional surface area, and F is the Faraday constant. According to the Nernst-Planck theory and assuming a pore transport pathway model, the steady-state flux of an ionic species (J_j) across a membrane during iontophoresis can be expressed as:

$$J_j = \varepsilon\left(-D_j\frac{dC_j}{dx} - z_j u_j C_j \frac{d\psi}{dx} \pm v_j C_j\right) \tag{4}$$

where ε is the combined effective porosity-tortuosity factor, ψ is the electric potential, v_j is the average effective velocity due to convection resulting from electroosmosis, and u_j, C_j, D_j, and x are, respectively, the effective electromobility, concentration, the effective diffusion coefficient, and the membrane position of the ionic species. In a charged membrane, the concentration of the ionic species in the membrane C_j is related to the concentration of the ionic species in the donor chamber $C_{j,D}$ by: $C_j = KC_{j,D}$, where K is the partition coefficient due to ion charge-to-membrane charge interactions.

The effective diffusion coefficient D_j and the effective electromobility u_j are related (in the ideal case) according to the Einstein equation of diffusion and mobility:

$$u_j = \frac{D_j F z_j}{R_{gas} T} \tag{5}$$

where R_{gas} is the gas constant and T is temperature. When the permeant molecular size is of the order of magnitude of

the membrane pore size, transport hindrance should be considered. The effective diffusion coefficient is related to the hindrance factor (H_j) and the free aqueous diffusion coefficient of the ionic species ($D_{0,j}$):

$$D_j = H_j D_{0,j} \tag{6}$$

The hindrance factor is a function of membrane pore size and permeant molecular size. Assuming hindered transport across cylindrical pores in the membrane, the hindrance factor H_j can be expressed as (14):

$$H_j = \frac{6\pi(1-\lambda_j)^2}{K_t} \tag{7}$$

where λ_j is the ratio of the permeant radius to the pore radius and K_t is:

$$K_t = \frac{9}{4}\pi^2\sqrt{2}(1-\lambda_j)^{-5/2}\left[1+\sum_{n=1}^{2} a_n(1-\lambda_j)^n\right] + \sum_{n=0}^{4} a_{n+3}\lambda_j^n \tag{8}$$

The coefficients a_n for K_t in Eq. (8) can be found in the literature (14). Similarly, permeant transport due to convection v_j across membrane pores of the same order of magnitude of the permeant molecular size can be expressed as:

$$v_j = W_j v_0 \tag{9}$$

where v_0 is the average velocity of the convective solvent flow and:

$$W_j = \frac{(1-\lambda_j)^2\left(2-(1-\lambda_j)^2\right)K_s}{2K_t} \tag{10}$$

$$K_s = \frac{9}{4}\pi^2\sqrt{2}(1-\lambda_j)^{-5/2}\left[1+\sum_{n=1}^{2} b_n(1-\lambda_j)^n\right] + \sum_{n=0}^{4} b_{n+3}\lambda_j^n \tag{11}$$

The coefficients b_n in Eq. (11) can be found in the literature (14).

From Eq. (4), the passive flux of a permeant across a membrane becomes:

$$J_j = -\varepsilon H_j D_{0,j}\frac{dC_j}{dx} \tag{12}$$

Transport Experiments: General Setup

Iontophoresis experiments were carried out in a well-stirred two-chamber side-by-side diffusion cell system as described previously (15). The effective diffusion area of the diffusion cells was around 0.2 cm^2, and each compartment of the diffusion cell had a 2-ml volume. The membrane was sandwiched between the two half-cells with the edge of the membrane sealed with paraffin. The diffusion cell was placed in a circulating waterbath at 36 ± 1°C. Two milliliters of PBS and 2 ml donor solution were then pipetted into the receiver and donor chambers, respectively. The activity of the radiolabeled permeant in the donor solution was around 4×10^4– 4×10^5 dpm/ml. During iontophoresis, a DC current was applied with a constant current iontophoretic device (Phoresor II Auto, Model PM 850, Iomed, Inc., Salt Lake City, UT) using Ag/AgCl (cathode in the donor) and Ag (anode in the receiver) as the driving electrodes. Samples were withdrawn from the donor and receiver chambers at predetermined time intervals (20 to 30 min). Typically, 20-μl aliquots were taken from the donor chamber, and the entire 2 ml were withdrawn from the receiver chamber and replaced with 2 ml of the fresh solution. At predetermined times during iontophoresis, the entire donor solution was also removed and replaced with fresh donor solution to prevent any significant changes in pH and in the composition of the donor solution due to ion transport and the formation of electrochemical products at the electrode. The maximum allowable change was 20% of the original composition and the interval of donor solution replacement was estimated using the Faraday equation. The duration of the iontophoresis experiments was approximately 1.5 to 3 h unless otherwise stated. Passive transport experiments were conducted in the same way without the application of the electric field. In all experiments, the donor and receiver samples were mixed with 10 ml of scintillation cocktail (Ultima Gold, Packard Instrument, Meriden, CT) and analyzed by a liquid scintillation counter (Packard TriCarb Model 1900TR Liquid Scintillation Analyzer). The flux (J) and permeability coefficient (P) were calculated at steady-state under sink conditions (receiver concentrations were <10% of the donor concentrations):

$$J = \frac{1}{A_D}\frac{\Delta Q}{\Delta t} \tag{13}$$

$$P = \frac{1}{C_D A_D}\frac{\Delta Q}{\Delta t} \tag{14}$$

where C_D is the concentration of the permeant in the donor chamber, and $\Delta Q/\Delta t$ is the slope of the cumulative amount of the permeant transported across the membrane into the receiver chamber *vs.* time plot. The amount of permeant transported across the membrane was determined by the radioactivity (in dpm) transported across the membrane and the specific activity (dpm/mol) of the radiolabeled permeant in the donor solution. The specific activity was determined by dividing the radioactivity of the permeant in the donor solution by the total concentration of both radiolabeled and non-radiolabeled permeant in the solution.

Characterization of the Ion-Exchange Membrane

Experiments to characterize the ion-exchange membrane were divided into two parts: uptake experiments and passive transport experiments. The uptake experiments were further divided into membrane weight (water uptake) and concentration (solute uptake) measurements. In addition to the uptake

and transport experiments, the electrical resistance and the thickness of the membrane were determined by a four electrode potentiostat system (JAS Instrumental System, Inc., Salt Lake City, UT) and a micrometer, respectively.

In the uptake experiments for membrane weight measurements, the membranes were equilibrated in the solutions of interest in screw-capped vials and shaken at room temperature for at least 2 days. Approximately 10 ml of the solution was used for each membrane in these experiments, and the size of the membrane was $\approx 1 \times 1$ cm. Two equilibrating solutions were studied: deionized distilled water and 0.15 M NaSA. After equilibration, the membranes were removed from the vials by tweezers and blotted briefly with Kimwipes tissue paper to remove the solution on the membrane surfaces. The wet membranes were quickly weighed. The membranes were then dried and weighed after drying. In the experiments with deionized water, the membranes were dried in an oven at around 60°C for several hours. The weight of the membranes was also determined after they were dried on the bench-top at room temperature overnight. After weighing the membranes, the same procedure (equilibrating, drying, and weighing) was repeated with the same membranes to assess reversibility and reproducibility. Because both drying methods (dried in the oven and dried on the bench-top overnight) provided essentially the same weight results with deionized water, only bench-top drying was carried out in the experiments when 0.15 M NaSA was the equilibrating solution.

In the solute uptake studies, SA was the probe to determine possible permeant charge-to-membrane charge interactions in the membrane, and urea and mannitol were to assess the effective porosity of the membrane. The general equilibration procedure in these solute uptake studies was the same as that in the weight measurement study, and 0.15 M NaSA was the equilibrating solution with trace amounts of ^{14}C-SA, ^{14}C-urea, or ^{3}H-mannitol. Immediately before and after equilibration, samples of the equilibrating solutions were taken to check for possible depletion of these compounds in the solutions during equilibration. The samples were mixed with 10 ml of the scintillation cocktail, and the concentrations of SA, urea, and mannitol were determined by liquid scintillation counting. It was found that the concentration of the equilibrating solution was essentially the same (less than 5% changes) before and after the equilibration period. In the experiments with ^{14}C-SA, the membranes were removed from the vials by tweezers at the end of the equilibration period, and the solution on the membrane surfaces was removed with Kimwipes tissue paper. The membranes were then equilibrated in separate vials of 0.2 ml PBS overnight with agitation for SA extraction. After extraction, the membranes were removed from the vials, and the solutions in the vials were mixed with 10 ml scintillation cocktail. The amounts of SA extracted from the membranes into the solutions were then assayed with the liquid scintillation counter. This procedure was repeated for subsequent extraction/equilibration with fresh PBS (0.2 ml in vials) until the amounts of SA extracted into PBS were less than 10% of the amounts in the first extraction. In the experiments with ^{14}C-urea and ^{3}H-mannitol, the membranes were mixed with 10 ml scintillation cocktail and equilibrated for at least 2 days with occasional agitation. The mixtures were then assayed by liquid scintillation counting. In a separate study, 0.015 and 1.0 M NaSA solutions were used as the equilibrating solutions with trace amounts of ^{14}C-SA to determine possible effects of NaSA concentration upon membrane SA uptake. For the lowest NaSA concentration (0.015 M), the equilibrating procedure was modified to using approximately 15 ml equilibrating solution per membrane and replacing the solution four times with fresh equilibrating solution.

Passive transport experiments with the ion-exchange membrane were conducted with SA, TEA, urea, and mannitol in the same side-by-side diffusion cell experimental setup as described in Transport Experiments: General Setup but without the application of an electric field. In these passive transport experiments, the donor solution was 0.15 M NaSA premixed with trace amounts of the radiolabeled permeants. The receiver solution was either 0.15 M NaSA or PBS. Preliminary transport experiments with the ion-exchange membrane were carried out over a period of at least 2 days (up to 5 days) to determine the time when steady-state transport would occur. It was found that a pre-equilibration step was necessary prior to the SA transport experiments because, without membrane pre-equilibration, the transport lag time of SA across the (oppositely charged) ion-exchange membrane was approximately 1 day. Therefore, before the SA transport experiments, the ion-exchange membrane was pre-equilibrated in the donor solution in a flask and stirred for at least 2 days. The volume of the equilibrating donor solution was approximately 10 ml per ion-exchange membrane. In the experiments of TEA, urea, and mannitol, the ion-exchange membranes were pre-equilibrated in 0.15 M NaSA as described above without the radiolabeled permeants before the transport experiments. The transport experiments were conducted with duration at least four times longer than the transport lag time.

The effective pore sizes of the membranes were determined as described previously (16–18). Briefly, the steady-state permeability coefficients of the membranes for permeants of different molecular sizes (i.e., urea and mannitol) were determined, and the ratios of the permeability coefficients of these permeants were calculated. The effective pore radii were then determined by the ratios of the permeability coefficients and the hindered transport equations in Theory and Equations. It should be noted that the effective pore radius is a parameter determined to characterize the barrier properties of the membrane. The transport pathways in the membranes are not necessarily cylindrical pores. Factors such as pore geometries are absorbed into the effective pore radius determined.

Characterization of the Sclera

Passive transport data of the sclera are abundant in the literature (15,19) and therefore such experiments were not repeated in the present study. In the present study, uptake experiments with sclera were performed to compare the properties of the sclera with those of the ion-exchange membrane. Both sclera with the retina and without the retina were used in these experiments. Sclera without the retina was prepared by carefully removing the retina layer from the sclera with a pair of forceps in tissue preparation before the experiments. The procedure of the uptake experiments was the same as that described in Characterization of the Ion-Exchange Membrane, except that the tissues were obtained in wet form (the ion-

exchange membrane was received dry). The tissues were initially weighed and dried on bench-top before they were used.

Iontophoretic Transport Across Ion-Exchange Membranes

As described in Characterization of the Ion-Exchange Membrane, the ion-exchange membranes were pre-equilibrated in the donor solution for at least 2 days prior to the transport experiments. The donor solution was prepared by mixing trace amounts of the radiolabeled SA with 0.15 M NaSA in deionized distilled water. After membrane equilibration, an assembly of one, two, or five ion-exchange membranes was sandwiched between the two diffusion half-cells. The receiver solution was PBS. Cathodal iontophoresis (cathode in the donor) of 0.4, 1, and 2 mA was carried out as described in Transport Expriments: General Setup.

Iontophoretic Transport Across Ion-Exchange Membranes in Series with the Sclera

The ion-exchange membrane was pre-equilibrated in the donor solution as described in Characterization of the Ion-Exchange Membrane. The donor and receiver solutions were prepared as described in Iontophoretic Transport Across Ion-Exchange Membranes. Then, one, two, or five ion-exchange membranes were assembled in series with the sclera and sandwiched between the two diffusion half-cells, with the ion-exchange membranes facing the donor chamber and the choroid side of the sclera facing the receiver chamber. Iontophoresis of 0.4, 1, and 2 mA was conducted as described in Transport Experiments: General Setup.

Assessment of Electroosmosis Across Ion-Exchange Membranes in Series with the Sclera

Cathodal iontophoresis experiments of urea and mannitol at 1 and 2 mA were conducted to determine the effects of electroosmosis across the assembly of the ion-exchange membrane in series with the sclera. Passive transport experiments without the application of an electric field were also performed and served as the baseline. The ion-exchange membrane was pre-equilibrated in 0.15 M NaSA solution prior to the transport experiments as described in Characterization of the Ion-Exchange Membrane but without any radiolabeled permeants. After membrane equilibration, an ion-exchange membrane was assembled in series with the sclera in the side-by-side diffusion cell as described in Transport Experiments: General Setup with the ion-exchange membrane facing the donor chamber and the choroid side of the sclera facing the receiver. Passive and iontophoresis experiments were then performed with radiolabeled urea and mannitol in 0.15 M NaSA in the donor chamber and PBS in the receiver chamber. The fluxes of urea and mannitol across the combined ion-exchange membrane-sclera system were determined.

To assess the contribution of electroosmosis, the Peclet numbers (Pe) were determined (18):

$$E = \frac{Pe}{1 - \exp(-Pe)} \tag{15}$$

where E is the enhancement factor due to electroosmosis, defined as the ratio of the permeability coefficient of iontophoretic transport to that of passive transport, assuming no electric field-induced alteration of the membranes. To calculate the apparent velocity of the convective solvent flow across the ion-exchange membrane by assuming the ion-exchange membrane as the transport-rate dominating barrier (shown to be a reasonable assumption later in this paper), the velocities (v_0) were calculated using the relationship:

$$Pe = \frac{Wv_0(\Delta x)}{HD_0} \tag{16}$$

where Δx is the effective thickness of the membrane (membrane thickness $\times$ tortuosity factor) and D_0 is the free diffusion coefficient. W and H are the hindered transport factors for convection and diffusion as described in Theory and Equations. The effective pore size of the transport pathway across the membrane assembly during passive and iontophoresis transport was determined as described in Characterization of the Ion-Exchange Membrane.

RESULTS

Ion-Exchange Membrane Characterization

Table I presents the weight of 1 cm^2 ion-exchange membranes (surface area ranging from 1.0 to 1.1 cm^2) and the uptake of urea, mannitol, and SA into the membranes. The physical thicknesses of the dry ion-exchange membranes and wet membranes equilibrated in 0.15 M NaSA were essentially the same and were approximately 0.05 to 0.06 cm. Therefore, the volume of the membranes was around 0.06 cm^3 relatively independent of membrane hydration. As can be seen in Table I, the wet weight of the membrane in equilibrium with distilled deionized water (66 ± 4 mg) was essentially the same as that equilibrated in 0.15 M NaSA solution (69 ± 4 mg). The amounts of water uptake into the membrane determined by the weight differences of 1 cm^2 wet and dry membranes were 13 and 15 mg in deionized water and 0.15 M NaSA solution, respectively. This corresponds to membrane porosity of approximately 0.2. Repeating the drying and equilibration treatments on the same membranes provided essentially the same weight results (data not shown), showing good reproducibility and membrane reversibility. The effective porosity of the membrane can also be determined using the urea and mannitol uptake data and the aqueous concentration of urea and mannitol in the equilibrating solution as previously described (20). The effective porosity volumes determined by urea and mannitol uptake were 0.011 ± 0.001 and 0.005 ± 0.001 ml, respectively (Table I), corresponding to effective porosity values of 0.16 for urea and 0.07 for mannitol. Thus, the effective porosity of the membrane determined using the weight of the ion-exchange membrane (i.e., water uptake) is larger than that determined by urea uptake, which in turn is larger than that by mannitol. This trend of decreasing membrane porosity (from water, urea, to mannitol) suggests that the sizes of the pores in the membrane are in the same order of magnitude of the sizes of the solutes, with increasing exclusion of solutes of higher molecular weight from the pores. Assuming cylindrical pore geom-

Table I. Properties of the Ion-Exchange Membrane (Ionac) and the Sclera (without the Retina)[a]

	Ionac, 1 cm^2	Sclera, 1 cm^2
Dry weight (mg)	53 ± 3	21 ± 6
Wet weight in water (mg)	66 ± 4	46 ± 11
Water content in water (mg)	13 ± 2	23 ± 6
Wet weight in 0.15 M NaSA (mg)	69 ± 4	63 ± 7
Water content in 0.15 M NaSA (mg)	15 ± 2	40 ± 6
Volume determined by urea uptake (μl)[b]	11 ± 1	47 ± 4
Volume determined by mannitol uptake (μl)[b]	5 ± 1	45 ± 5
Salicylate uptake in 0.15 M NaSA (M)[c]	4 ± 1	0.17 ± 0.01
Effective pore size (nm)[d]	0.8 ± 0.1	>5[e]
Electrical resistance in saline (kΩ cm^2)	0.11 ± 0.04	0.01 to 0.02
Physical thickness (cm)[f]	0.05 ± 0.01	0.03 to 0.05[g]

[a] Mean ± SD ($n \geq 3$).
[b] In 0.15 M NaSA.
[c] Total concentration calculated using the amount of SA and the volume of water in the membrane.
[d] Determined by urea and mannitol permeability coefficients in the transport experiments as described in the text.
[e] Effective pore size cannot be determined due to the limitation of the method used (21).
[f] Physical thickness of the membrane measured with a micrometer.
[g] Thickness of the sclera hemisphere is not uniform.

etry in the ion-exchange membrane, the effective radius of the pores in the membrane can be determined by the effective porosity values for urea and mannitol and the ratio of the partitioning function $(1 - \lambda_j)^2$ (see Eqs. 7 and 10) for the two permeants. The effective pore radius of the membrane estimated using this method was 0.7 nm.

In the equilibration study with 0.15 M NaSA, the amount of SA taken up into the membrane was approximately 0.06 mmol. The concentration of SA in the membrane determined by dividing this value with the amount of water in the membrane is approximately 4 M (Table I). This concentration value is significantly larger than that of the equilibrating solution (0.15 M) and is consistent with the high surface charge density of the membrane. If some pores in the membrane are accessible to water but not to SA due to size exclusion of the molecule, the microscopic SA concentration in the pores will be larger than the concentration determined above. To estimate this microscopic concentration, the amount of SA in the membrane was divided by membrane porosity volume for mannitol as mannitol and SA have similar molecular sizes. The microscopic concentration of SA in the membrane estimated by this method is approximately 12 M. It should be noted that membrane SA uptake was independent of the concentration of SA in the equilibrating solution in the present study. In the equilibrating solutions of 0.015 and 1.0 M NaSA, the amounts of SA taken up into the membrane were 0.06 and 0.07 mmol, respectively. The relative constant amounts of SA in the membrane in 0.015, 0.15, and 1.0 M NaSA suggest that the present equilibration procedure to replace the chloride ion originally in the membrane with SA was adequate.

Table II presents the passive permeation data of urea, mannitol, TEA, and SA across the ion-exchange membrane. Passive transport data of mannitol, TEA, and SA across the sclera obtained in previous studies (15,21) are also presented in the table for comparison. First, the data in the table show that the permeability coefficients of the ion-exchange mem-

Table II. Passive Transport of SA, Mannitol, TEA, and Urea Across the Ion-Exchange Membrane (Ionac) and the Sclera with Solutions of Sodium Salicylate (NaSA), Tetraethyl Ammonium Chloride (TEACl), or Phosphate Buffered Saline (PBS) in the Donor and Receiver Chambers

		Permeability coefficient (10^{-7} cm/s)[a]	Permeability coefficient (10^{-5} cm/s)[a]
Permeant	Condition (donor/receiver)	Ionac	Sclera
SA	0.15 M NaSA/0.15 M NaSA	56 ± 5	–
SA	0.15 M NaSA/PBS	94 ± 10	3.0 ± 0.9[c]
Mannitol	0.15 M NaSA/0.15 M NaSA	2.7 ± 0.3	–
Mannitol	0.15 M NaSA/PBS	4.4 ± 0.5	–
Mannitol	Saline/saline	–	2.6 ± 0.9[b]
Mannitol	PBS/PBS	–	2.2 ± 0.4[c]
Mannitol	0.15 M TEACl/PBS	–	2.5 ± 0.6[d]
TEA	0.15 M NaSA/0.15 M NaSA	0.036 ± 0.006	–
TEA	Saline/saline	–	3.5 ± 0.5[b]
TEA	0.15 M TEACl/PBS	–	3.6 ± 0.8[c]
Urea	0.15 M NaSA/0.15 M NaSA	28 ± 3	–
Urea	0.15 M NaSA/PBS	40 ± 2	–

[a] Mean ± SD ($n \geq 3$).
[b] (21).
[c] (15).
[d] Unpublished data.

brane for the permeants are significantly smaller than those of the sclera. For example, the permeability coefficient of the ion-exchange membrane for mannitol was two orders of magnitude smaller than that of the sclera. To determine the effective pore radius of the ion-exchange membrane, the permeability coefficients of urea and mannitol were compared. The ratio of the permeability coefficients of the ion-exchange membrane for urea and mannitol (11 ± 3) was around five times larger than the free aqueous diffusion coefficient ratio of urea and mannitol (2.0). Using the hindered transport theory in Theory and Equations, the effective pore radius of the pores in the ion-exchange membrane was determined to be 0.8 nm, which is significantly smaller than that of the sclera (>5 nm) determined in previous studies (21,22). The effective tortuosity of the ion-exchange membrane for mannitol transport was estimated using the effective membrane pore radius, effective membrane porosity for mannitol, passive mannitol permeability coefficient, and membrane thickness. This tortuosity value was around 2.

The ratio of the permeability coefficients of the ion-exchange membrane for TEA and mannitol (0.014 ± 0.004) and that for SA and mannitol (22 ± 4) in Table II are consistent with significant membrane pore charge influence on the transport of ionic permeants under the present ionic strength conditions. In contrast to the ion-exchange membrane, the permeability coefficients of the sclera for SA and TEA are essentially the same (last column, Table II), suggesting little or no significant pore charge-to-permeant charge interaction during transport. It is of interest to point out that the permeability coefficient of the ion-exchange membrane for SA under the condition of 0.15 M NaSA in both the donor and receiver chambers was lower (statistically significant but less than two times) than that when the donor and receiver solutions were, respectively, 0.15 M NaSA and PBS. The permeability coefficients of the neutral permeants mannitol and urea were both also lower to a comparable extent under the symmetric 0.15 M NaSA donor/receiver condition than when the donor/receiver condition was 0.15 M NaSA and PBS. The ratios of mannitol and SA permeability coefficients and those of mannitol and urea were not affected. A simple explanation for this is not apparent but these results do suggest a mechanism for the differing permeability coefficients under the NaSA/PBS and NaSA/NaSA conditions that would not involve significant changes in the effective membrane pore size and pore charge.

Characterization of the Sclera

Table I presents the sclera uptake data of water, urea, and mannitol for comparison with those of the ion-exchange membrane. The large amount of water in the sclera suggests that the sclera tissue has high porosity (>50%) consistent with the data reported previously with bovine and human sclera (23,24). Unlike the synthetic ion-exchange membrane, the water content of the sclera varies according to its surrounding environment, suggesting different degrees of swelling in solutions of different ionic strengths. For example, the weight of the tissue equilibrating in 0.15 M NaSA (63 ± 7 mg) was higher than that in deionized water (46 ± 11 mg). The initial weight of the sclera (wet weight in saline before the experiments, 70 ± 25 mg) was also higher than the weight of sclera in deionized water. Another difference between the ion-exchange membrane and the sclera is that the effective membrane porosities of the sclera are essentially same for water, urea, and mannitol. In 0.15 M NaSA, the effective porosity volume determined by tissue wet weight, urea uptake, and mannitol uptake was 0.040 ± 0.006, 0.047 ± 0.004, and 0.045 ± 0.005 ml, respectively (corresponding to porosity of approximately 0.6). This implies large effective membrane pore sizes with no significant size exclusion of the solutes from the pores in the tissue and is consistent with the pore size data in a previous transscleral transport study (21). Table I also presents the concentration of SA in the sclera. The total concentration of SA in the sclera is essentially the same as the aqueous concentration of SA in the equilibrating solution. This result suggests minimal SA binding to the sclera and is consistent with the previous conclusion of negligible pore charge-to-permeant charge interactions in transscleral transport (15,21).

The membrane uptake data in the present study also allow the characterization of the transport pathways in the sclera. A previous study estimated that the combined porosity–tortuosity factor ($\varepsilon = \varepsilon_0/\tau$) of the sclera was approximately 0.15 (15), where ε_0 and τ are the membrane porosity and tortuosity factors, respectively. Using the porosity data from Table I and the porosity–tortuosity factor in this previous study, the effective tortuosity of the sclera was determined to be around 4. This tortuosity value is consistent with the transport lag time (ranging from 10 to 20 min) observed in previous passive transscleral transport experiments (21).

Transport Across Ion-Exchange Membranes and Ion-Exchange Membranes in Series with the Sclera

Figure 1 shows the typical cumulative amount *vs.* time profiles in single experiments of SA transported across a stack of five ion-exchange membranes and five ion-exchange membranes in series with the sclera during 2 mA iontophoresis. Representative data of iontophoretic transport across the sclera without an ion-exchange membrane from a previous study (15) are also provided in the figure for

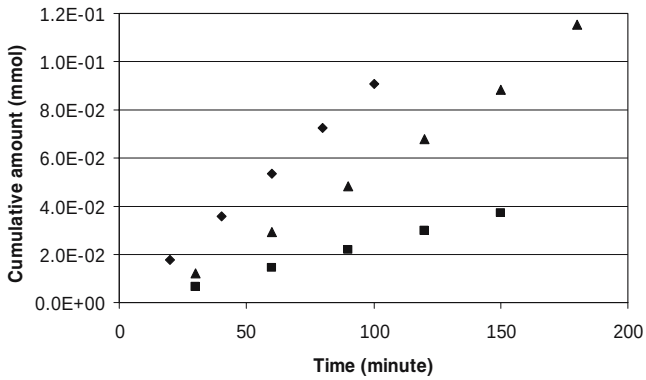

Fig. 1. Typical results of cumulative amount of SA transported across the membrane *vs.* time of five ion-exchange membranes, five ion-exchange membranes in series with the sclera, and the sclera alone during 2 mA cathodal iontophoresis. Symbols: *triangles*, five ion-exchange membranes in series with sclera; *diamonds*, five ion-exchange membranes; *squares*, sclera alone. The "sclera alone" data were taken from (15).

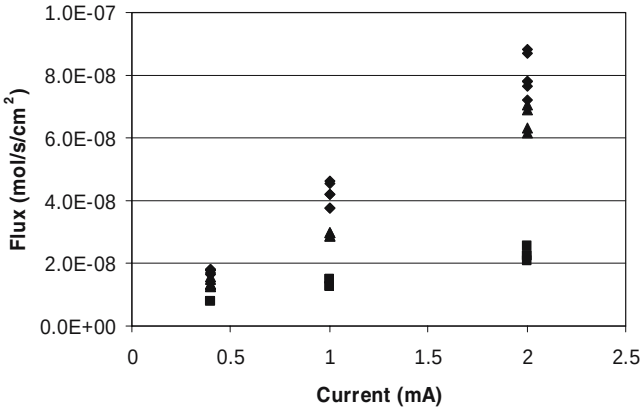

Fig. 2. Iontophoretic transport across an assembly of five ion-exchange membranes, five ion-exchange membranes in series with the sclera, and the sclera alone. The iontophoretic fluxes are plotted against the electric current applied across the membrane systems. Symbols: *triangles*, five ion-exchange membranes in series with sclera; *diamonds*, five ion-exchange membranes; *squares*, sclera alone. Each symbol represents the steady-state flux of a single iontophoresis run. The "sclera alone" data were taken from (15).

comparison. The data in the figure show steady-state transport across the membrane systems in the present study. The system of five ion-exchange membranes provided the highest flux during iontophoresis. The flux across the five ion-exchange membranes in series with the sclera was lower than that of the five ion-exchange membranes but higher than that across the sclera alone. In addition, the combined system of five ion-exchange membranes in series with the sclera showed the longest transport lag time.

To determine the transference numbers of SA in the present study, the steady-state fluxes of SA across the membrane systems during iontophoresis were first plotted against the applied electric current. Figure 2 shows the representative plots of steady-state SA fluxes *vs*. applied electric current for iontophoretic transport across an assembly of five ion-exchange membranes in series with sclera, five ion-exchange membranes, and the sclera. Using the slopes of the flux *vs.* electric current plots, the transference numbers of SA were determined with Eq. (3). Table III summarizes the slopes of the flux *vs*. electric current plots, their corresponding correlation coefficients (rsq), the transference numbers, and the normalized permeability coefficients of SA. As can be seen in the table, the flux *vs*. electric current slopes of one, two, and five ion-exchange membranes are significantly larger than those of one, two, and five ion-exchange membranes in series with the sclera ($p < 0.01$), which in turn are significantly larger than that of the sclera alone ($p < 0.01$). The slopes of the flux *vs*. electric current plots among the membrane systems of one, two, and five ion-exchange membranes are not statistically different from each other with ($p = 0.051$) or without ($p = 0.33$) stacked in series to the sclera. Statistical analyses were carried out using the statistical computing package SAS (Cary, NC) treating the steady-state flux in each individual experiment as a single data point.

Assessment of Electroosmosis Across Ion-Exchange Membrane in Series with the Sclera

Steady-state electroosmotic transport of the neutral model permeants mannitol and urea was observed during iontophoresis across an ion-exchange membrane in series with the sclera (Fig. 3). The observation of steady-state electroosmotic transport implies constant convective solvent flow with no continuous solution build-up in the membranes and at the membrane interface during iontophoresis in the present study. Table IV summarizes the urea and mannitol results. The permeability coefficients of urea and mannitol during iontophoresis were at least an order of magnitude smaller than those of SA (Table III); this suggests that the contribution of electroosmosis to ion-exchange membrane enhanced electrotransport was minimal. The enhancement factors presented in Table IV were calculated by dividing the 1 and 2 mA iontophoresis data by those of passive transport. The Peclet numbers (*Pe*) were then determined using the enhancement factors and Eq. (15). To estimate the velocities of the convective solvent flow across the ion-exchange membrane, the ion-exchange membrane was assumed to be the transport rate-dominating barrier, and the following parameters [in Eq. (16)] were first obtained. The *H* and *W* factors were calculated using the effective pore size in Table I and Eqs. (7)

Table III. Summary of the Transference Numbers of SA Determined in the Flux *vs.* Electric Current Plots of One, Two, and Five Ion-Exchange Membranes, One, Two, and Five Ion-Exchange Membranes in Series with Sclera, and Sclera Alone

Membrane assembly	Slope (Flux *vs.* Current; $\times 10^{-8}$ mol/s/cm^2/mA)[a]	rsq[b]	Transference number[c]	Permeability coefficient per mA (cm/s/mA)
1 Ionac	4.2 ± 0.1	0.999	0.81	2.8×10^{-4}
2 Ionac	4.2 ± 0.1	0.999	0.82	2.8×10^{-4}
5 Ionac	4.1 ± 0.1	0.994	0.78	2.7×10^{-4}
1 Ionac+sclera	3.5 ± 0.1	0.999	0.67	2.3×10^{-4}
2 Ionac+sclera	3.5 ± 0.1	0.995	0.68	2.3×10^{-4}
5 Ionac+sclera	3.3 ± 0.1	0.991	0.62	2.2×10^{-4}
Sclera[d]	1.1 ± 0.1	0.995	0.22	7.3×10^{-5}

[a] Slope of the flux (mol/s/cm^2) *vs.* current (mA) linear least squares regression with *y*-intercept fixed at the origin, from analyses of the steady-state fluxes in the 0.4, 1, and 2 mA experiments and treating each iontophoresis run as a single data point in a generalized linear model using SAS; regression slope ± standard error.
[b] rsq of the flux *vs.* current linear regression.
[c] Transference number calculated with the slope of the flux *vs*. current linear regression.
[d] Data taken from (15).

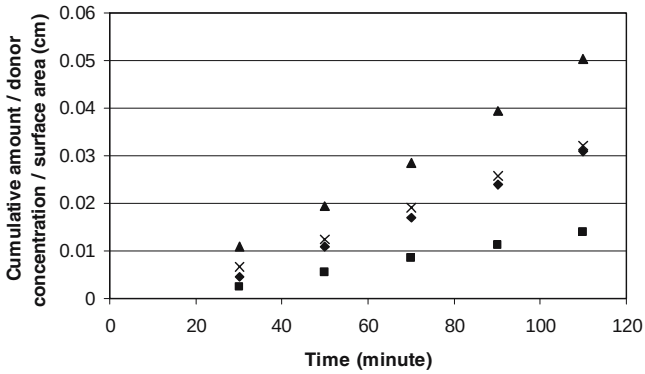

Fig. 3. Typical results of cumulative amount (normalized) transported across an ion-exchange membrane in series with the sclera *vs.* time during 1 and 2 mA cathodal iontophoresis. Symbols: *diamonds*, urea at 1 mA; *triangles*, urea at 2 mA; *squares*, mannitol at 1 mA; *crosses*, mannitol at 2 mA.

and (10). The effective thickness of the ion-exchange membrane (Δx; i.e., physical thickness × tortuosity) was assumed to be 0.1 cm. The convective solvent flow velocities across the ion-exchange membrane were then calculated using the *Pe* data, *H* and *W* factors, the effective thickness, and Eq. (16). These electroosmotic velocity values are presented in Table IV. The data show that the electroosmotic velocities for urea and mannitol are essentially the same and are proportional to the electric current, which is consistent with electrokinetic theory (25).

The effective pore size of the transport pathway across the assembly of ion-exchange membrane and sclera can also be determined using the ratios of the urea and mannitol permeability coefficients in passive and electroosmotic transport (Table IV). The effective pore radii determined using these data are around 0.7 nm. This value is essentially the same as that obtained in the passive transport study of the ion-exchange membrane alone without the sclera (0.8 nm), suggesting that the ion-exchange membrane is the transport rate-dominating membrane in passive and iontophoretic transport across the membrane assembly.

Also noted was the direction of the electroosmotic flow in these iontophoresis experiments that was from the cathode to the anode. A previous study has demonstrated that the transport pathway of the sclera is net negatively charged and transscleral electroosmosis (during iontophoresis) is from the anode to cathode (15); the permeability coefficients of sclera for mannitol during passive and anodal and cathodal iontophoresis of 2 mA were 2.2×10^{-5}, 7.0×10^{-5}, and 8.9×10^{-6} cm/s, respectively. When the sclera is placed against the ion-exchange membrane in the present study, the direction of electroosmosis across the sclera is reversed.

DISCUSSION

Sclera and Ion-Exchange Membranes

Recent advances in drug discovery and therapy of posterior eye diseases have stimulated new interest in the development of effective methods for drug delivery to the back of the eye. In transscleral iontophoresis, drug is delivered through the conjunctiva and the sclera into the eye with the assistance of an electric field. The sclera is relatively permeable with passive permeability coefficients in the range of 2 to 4×10^{-5} cm/s for small molecules. It has low electrical resistance in PBS and shows no transport hindrance due to the pore size of the membrane (15,21,27). The porous structure of the sclera also leads to relatively small transscleral iontophoretic flux enhancement (over passive transport) compared to biological membranes of lower porosities at the same applied electric current (15). However, it is the relatively high porosity of the sclera that makes significant ion-exchange membrane-enhanced iontophoresis possible.

The ion-exchange membrane has lower porosity than that of the sclera (Table I) and has more restrictive pores in which transport is significantly hindered due to molecular size exclusion. Both the porosity and effective pore size of the ion-exchange membrane contribute to the lower passive permeability coefficients of the membrane for SA, TEA, and mannitol than those of the sclera. The high charge density of the ion-exchange membrane, as evidenced by the SA uptake data, enhances the transport of SA and retards that of TEA. It is expected that the ion-exchange membrane is the rate- limiting barrier in drug transport across the assembly of the ion-exchange membrane and the sclera. In addition, electroosmosis across the ion-exchange membrane-sclera assembly occurs in the direction from the cathode to the anode during ionto-

Table IV. Permeability Coefficients, Enhancement Factors, Peclet Numbers, and Velocities of the Convective Solvent Flow Determined in the Iontophoresis and Passive Transport Experiments with Urea and Mannitol, and an Assembly of One Ion-Exchange Membrane and Sclera when 0.15 M NaSA and PBS were the Donor and Receiver, Respectively

	Urea			Mannitol		
	Passive	1 mA	2 mA	Passive	1 mA	2 mA
Permeability coefficient ($\times 10^{-6}$ cm/s)[a]	2.7 ± 1.0	6.4 ± 1.2	8.9 ± 1.0	0.4 ± 0.2	2 ± 1	4 ± 2
Enhancement factor[b]	–[e]	2.3 ± 0.3	3.3 ± 0.5	–[e]	4 ± 1	8 ± 3
Pe[c]	–[e]	2.0	3.2	–[e]	4	8
Velocity[d] ($\times 10^{-4}$ cm/s)	–[e]	1.2	1.9	–[e]	0.9	2

[a] Mean ± SD ($n \geq 5$).
[b] Enhancement factor determined by the passive and iontophoretic permeability coefficients.
[c] *Pe* numbers were calculated using the enhancement factor data and Eq. (15).
[d] Convective solvent flow velocity of electroosmosis was calculated using the *Pe* data and Eq. (16) and assuming effective thickness of 0.1 cm; transscleral electroosmosis without the ion-exchange membrane was in the opposite direction approximately 3×10^{-4} cm/s per mA (15) and when the thickness of the sclera was assumed to be 0.05 cm.
[e] Not applicable.

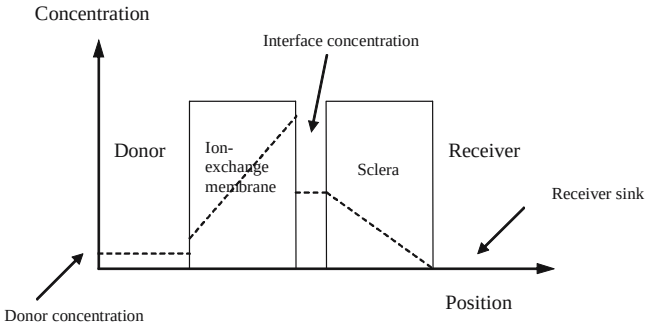

Fig. 4. Schematic diagram of the steady-state concentration gradients of SA predicted in the ion-exchange membrane-sclera assembly for iontophoretic transport of SA. The concentration gradients of Na ion are expected to be the same as those of SA (except in the ion-exchange membrane) to maintain charge neutrality in the system. In the ion-exchange membrane, the concentration of Na ion is lower than that of SA due to electrostatic effects on membrane partitioning. The concentrations of the buffer ions and Cl ion are low in the ion-exchange membrane-sclera assembly.

phoresis. The reversal of the direction of electroosmosis in the sclera in the presence of the ion-exchange membrane suggests that electroosmosis of the ion-exchange membrane supersedes that of the sclera. The essentially same effective pore size of the ion-exchange membrane-sclera assembly and that of the ion-exchange membrane alone (but not of the sclera alone) during passive and electroosmotic transport is additional evidence that the ion-exchange membrane is the rate-dominating barrier. Details of the mechanisms of ion-exchange membrane-enhanced electrotransport are discussed in what follows.

Mechanisms of Enhanced Transscleral Iontophoresis

Iontophoresis generally operates under three mechanisms: electroporation, electrophoresis, and electroosmosis (18,26,28). Electroporation is barrier alteration that increases the intrinsic permeability of the membrane. Electrophoresis is the facilitation of the movement of ionic species by the applied electric field, and electroosmosis assists the transport of both neutral and charged species by electric field-induced convective solvent flow. Due to the nature of the synthetic ion-exchange membrane and the collagen matrix in the sclera, electroporation is expected to be insignificant for iontophoretic transport across the membranes. Also, the urea and mannitol transport data in the present study show that electroosmosis contributes to less than 10% of the total iontophoretic flux of SA (Tables III and IV). The effects due to electroosmosis are therefore expected to be secondary. Intuitively, electrophoresis would consequently be the primary mechanism of enhanced transscleral iontophoresis under the experimental conditions in the present study, but a previous model simulation has shown significant contribution of diffusion to the total flux across an assembly of membranes of different barrier properties (13). According to the results of this model simulation, the higher intrinsic electromobilities (or intrinsic transference numbers) of SA in the ion-exchange membrane (than in the sclera) would lead to (a) high SA concentration at the interface between the ion-exchange membrane and the sclera and (b) large and opposing SA concentration gradients in the ion-exchange membrane and in the sclera (see Fig. 4). Diffusion of SA into the sclera driven by the high SA concentration at the interface enhances the transport of SA across the sclera but retards SA transport in the ion-exchange membrane. This balances the effects of the different intrinsic electromobilities of SA in the ion-exchange membrane and the sclera to provide the same total SA flux across the membrane system during iontophoresis at steady state. The observed iontophoretic transport enhancement can be primarily attributed to the net diffusion of SA in the sclera from the interface to the receiver via the high SA concentration at the interface. It should be pointed out that at higher applied electric current, higher SA concentration at the interface and higher contribution of diffusion to total flux are expected according to this model.

Significance of Enhanced Transscleral Iontophoresis in Drug Delivery

Typical iontophoresis has low transport efficiencies due to the relative high concentration of the endogenous competing counterions (e.g., NaCl) and the low electromobility of the drug ion compared with those of the endogenous counterions. The present study has demonstrated the utility of a synthetic ion-exchange membrane to enhance the efficiency of iontophoretic transport. Particularly, by placing the ion-exchange membrane on the sclera and excluding the transport of the current-carrying counterions from the receiver into the drug chamber, iontophoretic flux enhancement of SA was observed. A three-fold flux enhancement was achieved at steady state. Previous studies had proposed the use of ion-exchange membranes to enhance iontophoretic transport (12,29), but this method is most favorable in ocular iontophoresis because the ocular tissues (sclera/conjunctiva) have relatively low electrical resistance compared to other biological membranes. With the flux enhancement, (a) the same amount of drug can be delivered at lower applied electric current and/or shorter duration of iontophoresis treatment or (b) a larger amount of drug can be delivered at the same electric current and duration. This improvement will provide an opportunity of a superior iontophoresis system over existing conventional ocular iontophoresis methods. However, further studies are required to assess this improvement *in vivo*. During transscleral iontophoresis *in vivo*, the sclera is not the only transport barrier. Other barriers such as the conjunctiva, retinal epithelium, and retina are likely to be important. Blood vasculature clearance in the conjunctiva, choroid, and retina *in vivo* can also affect transscleral transport. Therefore, *in vitro* studies only serve as model systems and may not directly reflect transscleral iontophoresis in practice.

ACKNOWLEDGMENTS

This research was supported in part by NIH Grant EY015181. The authors thank Dr. Rajan P. Kochambilli for his help in the preparation of the experiments, Matthew S. Hastings and Dr. David J. Miller at Aciont Inc. (Salt Lake City, UT), Dr. Yanhui Zhang and Dr. Henry S. White for helpful discussion, Dr. Aniko Szabo and Dr. Lisa M. Pappas for their help in statistical analyses.

REFERENCES

1. G. B. Kasting. Theoretical models for iontophoretic delivery. *Adv. Drug Deliv. Rev.* **9**:177–199 (1992).
2. L. Hughes and D. M. Maurice. A fresh look at iontophoresis. *Arch. Ophthalmol.* **102**:1825–1829 (1984).
3. S. H. Yoo, D. Dursun, S. Dubovy, D. Miller, E. Alfonso, R. K. Forster, F. F. Behar-Cohen, and J. M. Parel. Iontophoresis for the treatment of paecilomyces keratitis. *Cornea* **21**:131–132 (2002).
4. F. F. Behar-Cohen, J. M. Parel, Y. Pouliquen, B. Thillaye-Goldenberg, O. Goureau, S. Heydolph, Y. Courtois, and Y. Kozak. Iontophoresis of dexamethasone in the treatment of endotoxin-induced-uveitis in rats. *Exp. Eye Res.* **65**:533–545 (1997).
5. F. F. Behar-Cohen, A. Aouni El, S. Gautier, G. David, J. Davis, P. Chapon, and J. M. Parel. Transscleral coulomb-controlled iontophoresis of methylprednisolone into the rabbit eye: influence of duration of treatment, current intensity and drug concentration on ocular tissue and fluid levels. *Exp. Eye Res.* **74**:51–59 (2002).
6. M. Voigt, M. Kralinger, G. Kieselbach, P. Chapon, S. Anagnoste, B. Hayden, and J. M. Parel. Ocular aspirin distribution: a comparison of intravenous, topical, and coulomb-controlled iontophoresis administration. *Invest. Ophthalmol. Vis Sci.* **43**:3299–3306 (2002).
7. T. M. Parkinson, E. Ferguson, S. Febbraro, A. Bakhtyari, M. King, and M. Mundasad. Tolerance of ocular iontophoresis in healthy volunteers. *J. Ocular Pharmacol. Ther.* **19**:145–151 (2003).
8. J. B. Phipps and J. R. Gyory. Transdermal ion migration. *Adv. Drug Deliv. Rev.* **9**:137–176 (1992).
9. B. H. Sage. Iontophoresis. In E. W. Smith and H. I. Maibach (eds)., *Percutaneous Penetration Enhancers*, CRC, Boca Raton, 1995, Ch 15.1.
10. M. B. Delgado-Charro and R. H. Guy. Iontophoresis of peptides. In B. Berner and S. M. Dinh (eds)., *Electronically Controlled Drug Delivery*, CRC, Boca Raton, 1998, Ch 7.
11. A. K. Banga and Y. W. Chien. Iontophoretic delivery of drugs: fundamentals, developments, and biomedical applications. *J. Control. Rel.* **7**:1–24 (1988).
12. S. P. Schwendeman, G. L. Amidon, V. Labhasetwar, and R. J. Levy. Modulated drug release using iontophoresis through heterogeneous cation-exchange membranes. 2. Influence of cation-exchanger content on membrane resistance and characteristic times. *J. Pharm. Sci.* **83**:1482–1494 (1994).
13. S. A. Molokhia, Y. Zhang, W. I. Higuchi, H. S. White, and S. K. Li. Iontophoretic transport across a multiple membrane system. In preparation.
14. W. M. Deen. Hindered transport of large molecules in liquid-filled pores. *AIChE J.* **33**:1409–1425 (1987).
15. S. K. Li, Y. Zhang, H. Zhu, W. I. Higuchi, and H. S. White. Influence of asymmetric donor-receiver ion concentration upon transscleral iontophoretic transport. *J. Pharm. Sci.* **94**:847–860 (2005).
16. K. D. Peck, A. H. Ghanem, and W. I. Higuchi. Hindered diffusion of polar molecules through and effective pore radii estimates of intact and ethanol treated human epidermal membrane. *Pharm. Res.* **11**:1306–1314 (1994).
17. S. K. Li, A. H. Ghanem, K. D. Peck, and W. I. Higuchi. Iontophoretic transport across a synthetic membrane and human epidermal membrane: a study of the effects of permeant charge. *J. Pharm. Sci.* **86**:680–689 (1997).
18. K. D. Peck, V. Srinivasan, S. K. Li, W. I. Higuchi, and A. H. Ghanem. Quantitative description of the effect of molecular size upon electroosmotic flux enhancement during iontophoresis for a synthetic membrane and human epidermal membrane. *J. Pharm. Sci.* **85**:781–788 (1996).
19. D. H. Geroski and H. F. Edelhauser. Transscleral drug delivery for posterior segment disease. *Adv. Drug Deliv. Rev.* **52**:37–48 (2001).
20. N. He, K. S. Warner, W. I. Higuchi, and S. K. Li. Model analysis of flux enhancement across hairless mouse skin induced by chemical permeation enhancers. *Int. J. Pharm.* **297**:9–21 (2005).
21. S. K. Li, S. A. Molokhia, and E. K. Jeong. Assessment of subconjunctival delivery with model ionic permeants and magnetic resonance imaging. *Pharm. Res.* **21**:2175–2184 (2004).
22. K. M. Hamalainen, K. Kananen, S. Auriola, K. Kontturi, and A. Urtti. Characterization of paracellular and aqueous penetration routes in cornea, conjunctiva, and sclera. *Invest. Ophthalmol. Vis Sci.* **38**:627–634 (1997).
23. D. M. Maurice and J. Polgar. Diffusion across the sclera. *Exp. Eye Res.* **25**:577–582 (1977).
24. T. W. Olsen, H. F. Edelhauser, J. I. Lim, and D. H. Geroski. Human scleral permeability. Effects of age, cryotherapy, transscleral diode laser, and surgical thinning. *Invest. Ophthalmol. Vis Sci.* **36**:1893–1903 (1995).
25. S. M. Sims, W. I. Higuchi, V. Srinivasan, and K. D. Peck. Ionic partition coefficients and electroosmotic flow in cylindrical pores: comparison of the predictions of the Poisson-Boltzmann equation with experiment. *J. Colloid Interface Sci.* **155**:210–220 (1993).
26. G. B. Kasting and J. C. Keister. Application of electro-diffusion theory for a homogeneous membrane to iontophoretic transport through skin. *J. Control. Release* **8**:195–210 (1989).
27. M. R. Prausnitz and J. S. Noonan. Permeability of cornea, sclera, and conjunctiva: a literature analysis for drug delivery to the eye. *J. Pharm. Sci.* **87**:1479–1488 (1998).
28. S. K. Li, A. H. Ghanem, K. D. Peck, and W. I. Higuchi. Pore induction in human epidermal membrane during low to moderate voltage iontophoresis: a study using AC iontophoresis. *J. Pharm. Sci.* **88**:419–427 (1999).
29. D. F. Untereker, J. B. Phipps, P. T. Cahalan, and K. R. Brennen. Iontophoresis electrode. US Patent 5,395,310 (1995).